The Analysis of Seismic Response for Base-isolated Structure by LS-DYNA

Song Zhenxia[1] and Ding Haiping[2]

[1] *PH D Candidate, Jiangsu Key Laboratory of Structure Engineering, Science and Technology University of Suzhou, China*

[2] *Prof, Jiangsu Key Laboratory of Structure Engineering, Science and Technology University of Suzhou, China*
Email:zx_song@163.com，hpding@126.com

ABSTRACT: LS-DYNA, a popular large-scale explicit finite element analysis software, adopt viscous boundary to simulate the effects of infinite field. It can solve the problems of SSI more effectively and conveniently. But because the precision of the viscous boundary is not high enough, viscous-spring boundary is introduced to substitute for viscous boundary. As demonstrated by numerical calculation results, this approach can improve the calculating precision obviously. A 7-storied base-isolated frame structure is analyzed with improved LS-DYNA in this paper, and essential models are established to compare the seismic responses of fixed base and base-isolated structures under 8 degree frequently and 8 degree rarely seism with SSI.

KEYWORDS: finite element, LS-DYNA, numerical simulation, SSI, base-isolated

1. INTRODUCTION

As an important aseismic measure for engineering structure, base isolation technology has attracted more and more concentration in recent decades. And it has been adopted by national code for design of building. Because the current aseismic theories are mostly based on assumption of rigid foundation, the influence of the soil-structure interaction (SSI) on base-isolation is often ignored in common theory analysis. Under the actual earthquakes, the flexibility and infinity of the soil will lead to magnitude differences between the model basing on rigid assumption and the whole system including soil, foundation and structure. Moreover, when the soil, foundation and structure are analyzed as a whole, the characteristic of input earthquake motion is different with that of rigid base. This paper does finite element analysis on whole seismic response of the base-isolated structure and the influence on isolated-structure of SSI is discussed.

The study on SSI problem include: structures, foundation, coupling of structure and foundation, and the infinite soil. Hitherto many general finite element soft wares have been programmed to solve the problem. But the analysis software often attends to one thing and loses another in dealing with SSI problem. For instance FLUSH, SASSI, etc are inconvenience because lacking of pre- and post- processors, and they can't consider the nonlinear of structure. The other software, such as SAP, ADINA, etc, even they have powerful pre- and post-processors and can analyze the nonlinear problems, but they can't simulate the radiation damping of infinite soil. The soil-structure system is a closed system that the ignoring of the artificial boundary condition lead to incorrect results. LS-DYNA is advanced in prep- and post- processor by ANSYS Company and adopts Non-Reflecting Boundary (viscous boundary) to simulate the effects of infinite ground. It can solve the SSI problems more effectively and conveniently. But because the precision of the viscous boundary is not high enough, viscous-spring boundary is introduced to substitute for viscous boundary in this paper. As demonstrated by numerical calculation results, this approach can improve the calculating precision obviously.

2. THE ARTIFICIAL BOUNDARY IN LS-DYNA AND THE IMPROVEMENT

When analyzing SSI problem by using the finite element method (FEM), the finite domain is cut out for simulating the interaction in infinite soil. The artificial boundary condition (ABC) will be constructing to absorb the energy of the scattering waves, from the generalized structure to the infinite media. This is the key problem in simulating of the SSI problems. There are some artificial boundaries in use: viscous boundary (Lysmer and Kulemeyer, 1969), superposition boundary (smith, 1974), paraxial approximate boundary (Foreman, 1986; Higdon, 1986; Keys, 1985), transmitting boundary (Liao, 1996), viscous-spring boundary (Deeks and Randolph, 1994). The viscous boundary considers only the absorption of energy from scatter waves. But because being easily realized in program, the viscous boundary was widely applied due to its clearly presented concept and convenient implementation earlier.

The basic idea of the viscous boundary is utilize the stress on boundary to simulate the influence of artificial boundary. The definition of stress on the boundary is as following:

$$\begin{aligned} \sigma_{normal} &= -\rho c_d v_{normal} \\ \sigma_{shear} &= -\rho c_s v_{\tan} \end{aligned} \tag{2.1}$$

Where ρ is the mass density. c_d and c_s are P wave velocity and SV wave velocity. v_{normal} and $v_{\tan}$ are the normal velocity and tangential velocity of the boundary. σ_{normal} and σ_{shear} are the normal and tangential stress of the boundary.

From physical concepts, a mechanical model with a viscous boundary is a separated body, which is suspended in space. The entire model can shift as a rigid body under low frequency force. To overcome the disadvantage of low precision and shifting under low-frequency, Deeks and Randolph (1994) presented a 2D viscous-spring boundary by deducing the equation in 2D cylindrical wave. Liu etc (2006) presented the 3D viscous-spring boundary by deducing the equation in 3D spherical wave. Equivalently, the ABC mentioned above can be installed continual parallel connection spring and damper system on artificial truncation boundary. The equations of the elastic coefficient K_b of spring and the damp coefficient C_b of damper are as following:

$$K_b = \alpha G / r_b \qquad C_b = \rho c \tag{2.2}$$

Where ρ and G are mass density and shear modulus of the medium; r_b is the distance between scatter source and artificial boundary; c is the wave velocity in medium, the value of parameter α is determined by the type of artificial boundary, refer to Table 1. If ignore the spring, this artificial boundary will degenerate to the viscous boundary. For improving the precision of LS-DYNA in analyzing the SSI problem, viscous-spring boundary is introduced to substitute for viscous boundary. The following paper will illuminate the enhancement of precision in improved LS-DYNA by two examples.

Table 1 The value of parameter α in viscous-spring artificial boundary

Type	Direction	α
2D artificial boundary	Normal in plane	2.0
	Tangential in plane	1.5
	Tangential out of plane	0.5
3D artificial boundary	Normal	4.0
	Tangential	2.0

For verifying the accuracy and reliability of viscous-spring artificial boundary condition in LS-DYNA, this paper adopts two examples in infinite or semi-infinite medium.

2.1. Inner-source Problem

Consider a homogeneous and isotropic infinite space with a vertical face force of $p(t)$ function on a surface in the model, as shown in Eqn.2.3. The load $p(t)$ is a pulse force, Equation is as:

$$p(t)=16\times10^{8}[G(t)-4G(t-1/4)+6G(t-1/2)-4G(t-3/4)+G(t-1)] \tag{2.3}$$

Where

$$G=(t/T_0)^3 H(t/T_0) \tag{2.4}$$

$$\begin{cases} H(t)=0, & t<0 \\ H(t)=1, & t\geq 0 \end{cases} \tag{2.5}$$

In upper equation, $H(t)$ is Heaviside ladder function, T_0 is sustained time, in this example $T_0=0.1s$, the wave shape is shown in Fig.1.

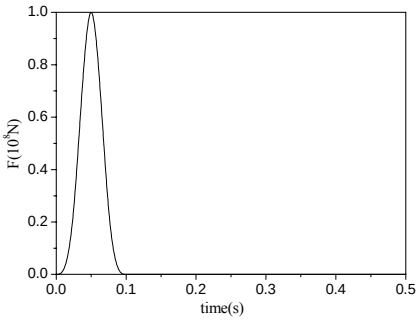

Figure 1 Load of $p(t)$

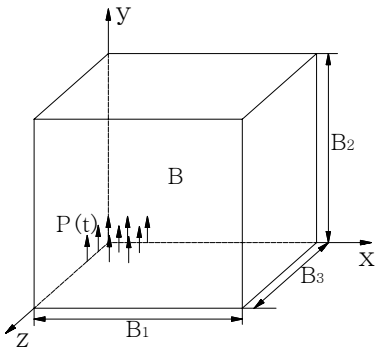

Figure 2 Inner-source model（the first quadrant）

In this example the range of the numerical computed object takes a cubic volume $80\times80\times80m$, the model in first quadrant is shown in Fig.2, where the parameter $B_1=B_2=B_3=40m$. The distributed force source $p(t)$ is in $-10\leq x,z\leq10m$ and on plane $y=0$. The grid size of $\Delta X=\Delta Y=\Delta Z=1m$ which is determined by the precision of the wave finite element simulate. The time interval $\Delta t=0.001s$ is used for this example which is determined by stability of numerical integral. The mass density $\rho=2000kg/m^3$, the shear wave velocity $c_s=200m/s$, the elastic module $E=2E8N/m^2$, the Poisson's ratio $\mu=0.25$. The artificial boundaries are far-fixed boundary, viscous boundary and viscous-spring boundary respectively, and the far-fixed boundary is the accurate solution of the problem because the reverberation on boundary of the wave has not reached the observed point. In LS-DYNA software, only need to select the nodes on boundary and definite the NON-REFLECTING-BOUNDARY condition, the artificial boundary is viscous boundary. For improving the viscous boundary to viscous-spring boundary, the springs are added to nodes in three directions. In simulating field, node A(0,0,0) and B(7,7,7) are observing points, the results are shown in Fig.3.

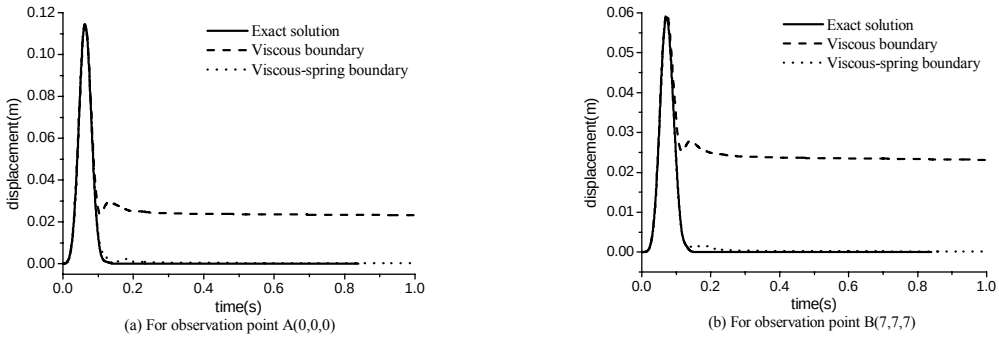

Figure 3 Displacement time history of the inner-source problem

2.2. Scatter Problem

In this example, consider a homogeneous and isotropic infinite semi-space with a vertical shear wave input $p(t)$ function on the bottom in the model. The range of the numerical computed object takes a cubic volume $80\times 80\times 40m$, the model in first quadrant is shown in Fig.4, where the parameter $B_1 = B_2 = B_3 = 40m$. The grid size ΔX=ΔY=ΔZ=2m. The time interval Δt=0.005s is used for this example which is determined by stability of numerical integral. The mass density $\rho = 2000kg/m^3$, the shear wave velocity $c_s = 100m/s$, the elastic module $E = 5E7N/m^2$, the Poisson's ratio $\mu = 0.25$. The artificial boundaries are far-fixed boundary, viscous boundary and viscous-spring boundary respectively. In simulating field, node A(0,0,0) and B(0,20,0) are observing points, the results are shown in Fig.5.

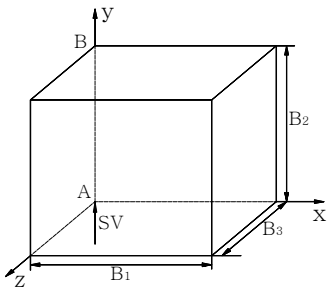

Figure 4 Scatter model（quarter）

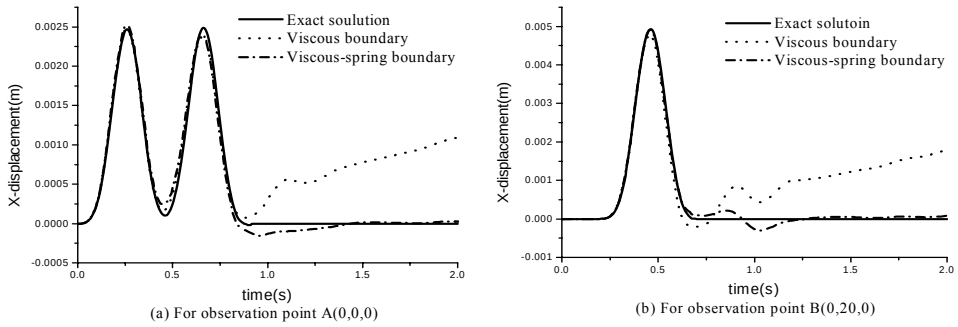

Figure 5 Displacement time history of the scatter problem

The numerical examples demonstrate that the viscous-spring boundary is better than viscous boundary. By using the proposed viscous-spring boundary in LS-DYNA, high numerical precision and adequate stability can be achieved. And the improved boundary condition overcomes the disadvantage of drifting in viscous boundary.

3. COMPUTATION AND ANALYSIS

3.1. Project Introduction

The Anti-seismic Center Synthetical Building in Yunnan Province is a 7-storied base-isolated reinforced concrete frame building lies in the southwest of Kunming City. The first floor is 3.9m high and the other floors are 3.2m high. The dimension of foundation is $35.4m\times 1m\times 10.8m$ (as shown in Fig.6). The dimension of the

beams section is $300 \times 500mm$, and the columns section is $600 \times 600mm$. The Young's Modulus of the beam and column is $E = 2.8E10N/m^2$ and $3.0E10N/m^2$, respectively.

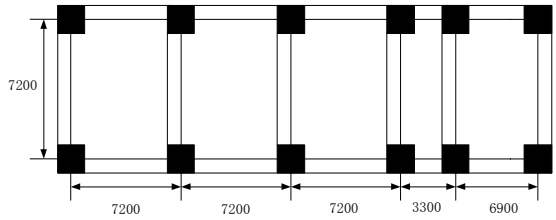

Figure 6 Structure Plan

In the project, the laminated rubber bearings (LRB), produced by Rubber Product Institute of Yunnan province, were located on the top of the basement so as to support the upper structure (the mechanical performance of the LRB refers to the Table 2). The plane layout of LRB is shown in Fig.7.

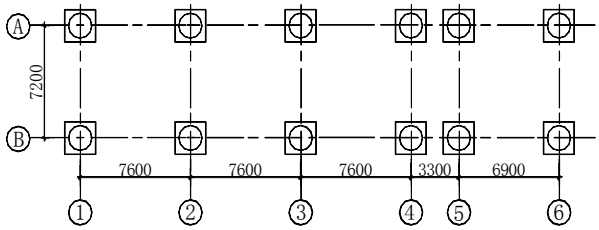

Figure 7 The plane layout of LRB

Table 2 The mechanical performance of LRB

Item	Unit	Laminated rubber bearings	
Type (Diameter)	mm	500	600
Height	mm	120	150
Diameter of lead core	mm	65	65
First shape factor	——	23.9	18.56
Second shape factor	——	7.4	6.19
Design bearing capacity	KN	2940	4240
Vertical stiffness	KN/mm	1960	2227
Horizontal stiffness	KN/mm	1.43	1.53
Equivalent viscous damp ratio	%	21.3	23.3

3.2. Modeling and Computation Methodology

3.2.1 Element model of laminated rubber bearings

LRB are simulated with spring and damper elements respectively which are fixed between the bottom and the foundation. The hysteretic framework curves of LRB have little change and its dynamical characteristic is quite stable under horizontal and repeated load which is alternate in positive and negative directions. Bilinear hysteretic model (as shown in Fig.8) can well simulate the hysteretic characteristics of isolation layers. In this

paper the bilinear hysteretic model of LRB was joined with program LS-DYNA using the design language of ANSYS. Thus the nonlinear simulation of materials can be realized.

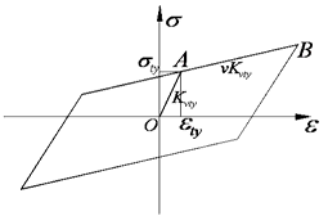

Figure 8 Bilinear hysteretic model

Where in Fig.8, point A is the yield point, OA is the first stiffness in elastically segment, the stress and strain of point A is yield stress and yield strain. When the pulling force exceeds the yield stress, the curve enters in to AB non-linearity segment, point B is unloading point, and AB is the second stiffness in non-linearity segment. The parameter ν is non-linearity stiffness coefficient, which denotes the reduction of stiffness when it is draught. $\nu = 0.06$.

3.2.2 Modeling of structure

For comparing the difference between base-isolated and non-base-isolated buildings, the frame structure model is established first. Then raft foundation is established and linked on the bottom of the columns, this is the non-base-isolated analysis model. When the LRB elements are inserted between the bottom columns and the base, it becomes the base-isolated model. If considering the SSI, the soils under the foundation are divided into two types: the upper soil is 28m thick, $E = 80E7N/m^2, \mu = 0.25, \rho = 2000kg/m^3, c_s = 400m/s$; the lower soil is 9m thick, $E = 137.5E7N/m^2$, $\mu = 0.25$, $\rho = 2200kg/m^3, c_s = 500m/s$. In the simulating model, the distance between the boundary of soil and the columns on edge is 18m. The dimension of soil is $67.8m \times 37m \times 43.2m$. The zero is the crossing point of left column and foundation. The artificial boundary adopt viscous-spring boundary. (as shown in Fig.9)

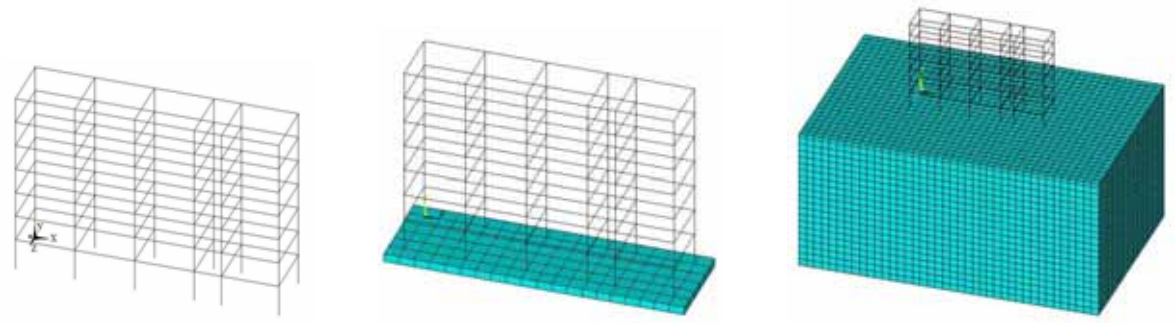

(a) Frame model (b) Model without SSI (c) Model with SSI

Figure 9 The model of simulation analysis

3.2.3 Input seismic waves

A real seismic wave record and an artificial seismic wave are adopted in this paper. The real seismic wave is the horizontal earthquake record in Kunming and another is artificial seismic wave, and is adjusted according to accelerations of 8 degree frequently and rarely occurred earthquake in Code for seismic design of buildings. The frequently accelerations of the seismic waves are shown in Fig.10. When considering SSI effect the

earthquake wave is at bedrock. Therefore the input accelerations at bedrock should be inversed from ground motions.

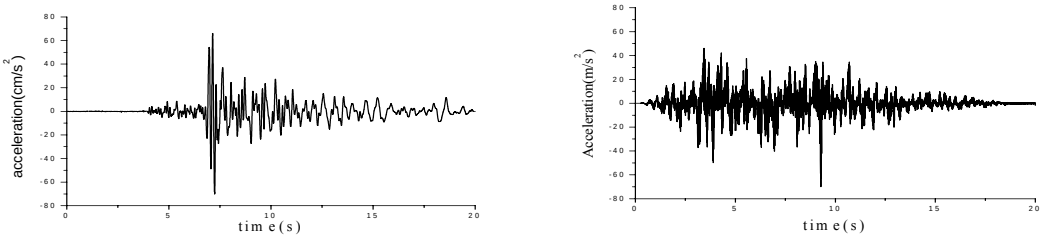

(a) Real earthquake record (b) Artificial seismic wave

Figure 10 Ground acceleration history (frequently occurred earthquake)

3.3. Analyses of the Results

Fig.11 to Fig.12 show the inter-laminar displacements in frequently and rarely occurred earthquake, respectively.

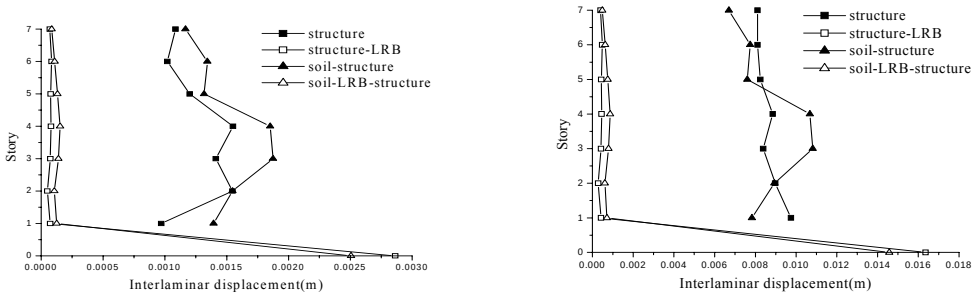

(a) 8 degree frequently earthquake (b) 8 degree rarely earthquake

Figure 11 Real earthquake

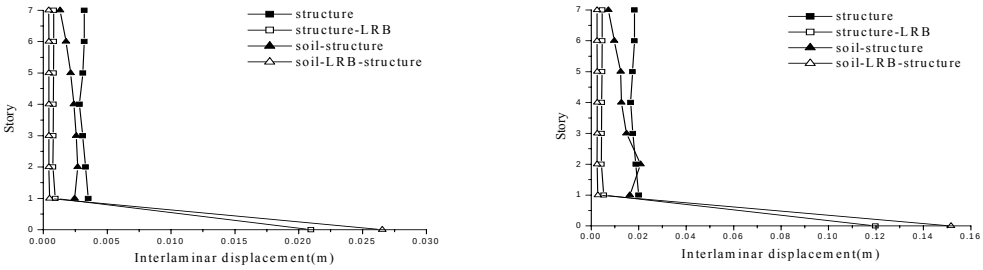

(a) 8 degree frequently earthquake (b) 8 degree rarely earthquake

Figure 12 Artificial earthquake

From the figures, we can find that when adopting the LRB, the amplitude of inter-laminar displacements reduced greatly whether considering the SSI or not. Under the real seism, when considering SSI the changes of the inter-laminar displacements of non-base-isolated structure increased in frequently earthquake, but reduced in rarely earthquake sometimes. The amplitude of inter-laminar displacement of base-isolated structure amplified with SSI than the case of without SSI in frequently and rarely earthquake. Under the artificial seism, the inter-laminar displacements reduced when considering the SSI in frequently and rarely earthquakes.

4. CONCLUSIONS

1. The viscous-spring boundary is introduced to substitute for viscous boundary in LS-DYNA software. As demonstrated by numerical calculation results of typical examples, this approach can improve the calculating precision obviously, and by using the viscous-spring artificial boundary, simulating wave motion and the soil-structure interaction in the infinite and semi-infinite medium is effective, accurate and convenient.

2. By establishing the SSI and without SSI models to compare the influence of soil-structure interaction to fixed base and base-isolated structure, this paper draws out some useful and significance conclusions. The capability of isolation system is nearly correlative with ground soil. Therefore it is necessary to study the influence of soil-structure dynamic interaction on base isolation in the research of isolation system. It is more reasonable with the fact and more instructional for the real-life project to analyze whole seismic response of the structure, isolation layers and soil.

In addition, the non-linearity of the soil is not considered in the paper. When this case is considered, the results may change especially in major earthquake and this is our future work.

ACKNOWLEDGEMENT

This research is supported by the Jiangsu Provincial Fund of Key Subject of Structure Engineering.

REFERENCE

John, O. Hallquist. (1998). ANSYS/LS-DYNA3D Theoretical Manual, Livemore Software Technology Corporation.

Zhang, D.Y, Jin, X. and Ding, H. P. (2005). The use of ANSYS/LS-DYNA in earthquake engineering. *Earthquake Engineering and Engineering Vibration* 25:4, 170-174 (In Chinese)

Lysmer J and Kulemeyer R. L. (1969). Finite dynamic model for Infinite media. *Journal of Engineering Mechanics,* ASCE 95: 759-877.

Smith W. D. (1974). A nonreflecting plane boundary for wave propagation problems. *Journal of Computational Physics* 15:4, 492-503.

Foreman M.G. (1986). An accuracy analysis of boundary conditions for the forced shallow water equations. *Journal of Computational Physics* 64, 334-367.

Liao, Z.P. (1996). Extrapolation nonreflecting boundary conditions. *Wave Motion*, 24, 117-138. (In Chinese)

Deeks, A. J. and Randolph, M. F. (1994). Axisymmetric Time-domain Transmitting Boundaries. *Journal of Engineering Mechanics* 120:1, 25-42.

Liu, J.B and Du, Y.X, etc. (2006). 3D spring-viscous artificial boundary in time domain. *Earthquake Engineering and Engineering Vibration* 5:1, 93-102

Lysmer, J. and Drake, L.A. (1972). A finite element method for seismology. *Methods in Computational Physics. Academic Press, New York*, 181-216.

Liao, Z.P. (2002). Introduction to wave motion theories in engineering, *China Academic Press*, Beijing. (In Chinese)